National Aeronautics and
Space Administration

Lyndon B. Johnson Space Center

Recent Advancements in Fully Implicit Numerical Methods for Hypersonic Reacting Flows

with Application to Reentry and Arcjet Modeling

Benjamin S. Kirk[†], Roy H. Stogner[⋆],
Todd A. Oliver[⋆], and Paul T. Bauman[⋆]

[†] NASA Lyndon B. Johnson Space Center, USA
[⋆] Institute for Computational Engineering & Sciences – The University of Texas at Austin, USA

September 26, 2012

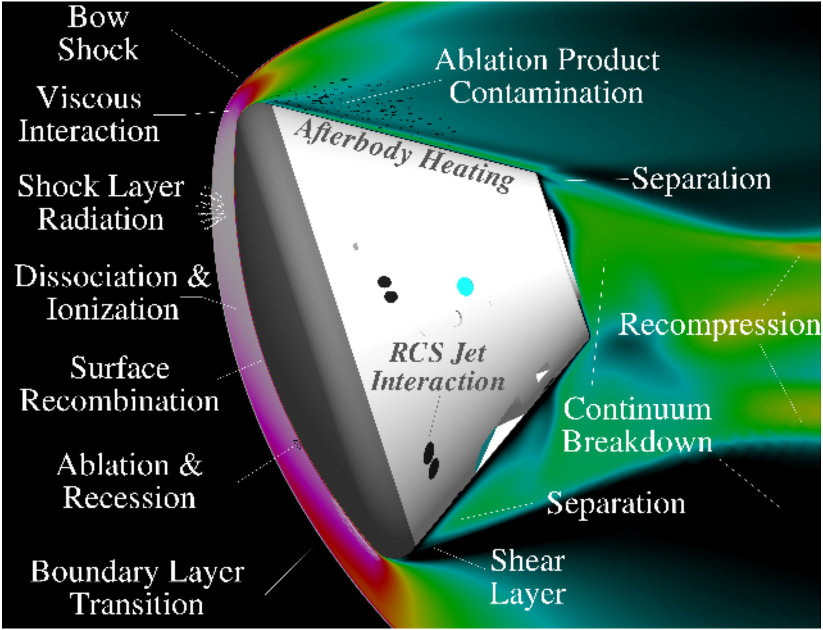
Bow Shock
Viscous Interaction
Shock Layer Radiation
Dissociation & Ionization
Surface Recombination
Ablation & Recession
Boundary Layer Transition
Ablation Product Contamination
Afterbody Heating
Separation
Recompression
RCS Jet Interaction
Continuum Breakdown
Separation
Shear Layer

- When chemical kinetic timescales are approximately equal to flow timescales, the chemical composition of a flowfield must be determined as part of a simulation procedure. Such flows are in *chemical nonequilibrium*.

- When chemical kinetic timescales are approximately equal to flow timescales, the chemical composition of a flowfield must be determined as part of a simulation procedure. Such flows are in *chemical nonequilibrium*.

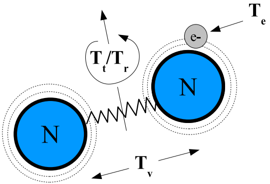

- Molecules and atoms can store energy in various *modes*.
- At hypersonic conditions these modes may not be in equilibrium, resulting in *thermal nonequilibrium*.

- When chemical kinetic timescales are approximately equal to flow timescales, the chemical composition of a flowfield must be determined as part of a simulation procedure. Such flows are in *chemical nonequilibrium*.

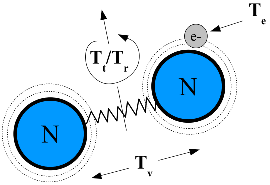

- Molecules and atoms can store energy in various *modes*.
- At hypersonic conditions these modes may not be in equilibrium, resulting in *thermal nonequilibrium*.

- The physical models and governing equations for flows in thermochemical nonequilibrium have been simulated previously with finite difference and finite volume techniques.
- In this work we review the physical models and implement a SUPG finite element scheme for hypersonic flows in thermochemical nonequilibrium.

- At hypersonic entry conditions, surface temperatures may exceed capabilities of reusable thermal protection system materials.
  - Reusable materials typically limited to $T < 2,000\,\text{K}$.
  - It is necessary then to consider *ablative materials*.

- At hypersonic entry conditions, surface temperatures may exceed capabilities of reusable thermal protection system materials.
  - Reusable materials typically limited to $T < 2,000\,\mathrm{K}$.
  - It is necessary then to consider *ablative materials*.
- Ablative materials respond to high temperatures through pyrolysis, decomposition, blowing, and surface recession.
- Typically, ablation analysis is decoupled from the external flowfield, but we hope to do better.
- Additionally, accurately characterizing ground test facilities requires increased fidelity.

- At hypersonic entry conditions, surface temperatures may exceed capabilities of reusable thermal protection system materials.
  - Reusable materials typically limited to $T < 2,000\,\mathrm{K}$.
  - It is necessary then to consider *ablative materials*.
- Ablative materials respond to high temperatures through pyrolysis, decomposition, blowing, and surface recession.
- Typically, ablation analysis is decoupled from the external flowfield, but we hope to do better.
- Additionally, accurately characterizing ground test facilities requires increased fidelity.

- As we will see, however, more accurate numerical modeling results in unique numerical challenges, necessitating novel numerical algorithms.

- At hypersonic entry conditions, surface temperatures may exceed capabilities of reusable thermal protection system materials.
  - Reusable materials typically limited to $T < 2,000\,\mathrm{K}$.
  - It is necessary then to consider *ablative materials*.
- Ablative materials respond to high temperatures through pyrolysis, decomposition, blowing, and surface recession.
- Typically, ablation analysis is decoupled from the external flowfield, but we hope to do better.
- Additionally, accurately characterizing ground test facilities requires increased fidelity.

- As we will see, however, more accurate numerical modeling results in unique numerical challenges, necessitating novel numerical algorithms.

Governing Equations

- Extension from a single-species calorically perfect gas to a reacting mixture of thermally perfect gases requires species conservation equations and additional energy transport mechanisms.

$$
\begin{aligned}
\frac{\partial \rho}{\partial t} + \boldsymbol{\nabla} \cdot (\rho\, \boldsymbol{u}) &= 0 \\
\frac{\partial \rho \boldsymbol{u}}{\partial t} + \boldsymbol{\nabla} \cdot (\rho \boldsymbol{u} \boldsymbol{u}) &= -\boldsymbol{\nabla} P + \boldsymbol{\nabla} \cdot \boldsymbol{\tau} \\
\frac{\partial \rho E}{\partial t} + \boldsymbol{\nabla} \cdot (\rho H \boldsymbol{u}) &= -\boldsymbol{\nabla} \cdot \dot{\boldsymbol{q}} + \boldsymbol{\nabla} \cdot (\boldsymbol{\tau} \boldsymbol{u})
\end{aligned}
$$

Governing Equations

- Extension from a single-species calorically perfect gas to a reacting mixture of thermally perfect gases requires species conservation equations and additional energy transport mechanisms.

$$
\begin{aligned}
\frac{\partial \rho_s}{\partial t} + \boldsymbol{\nabla} \cdot (\rho_s \boldsymbol{u}) &= \boldsymbol{\nabla} \cdot (\rho \mathcal{D}_s \boldsymbol{\nabla} c_s) + \dot{\omega}_s \\
\frac{\partial \rho \boldsymbol{u}}{\partial t} + \boldsymbol{\nabla} \cdot (\rho \boldsymbol{u}\boldsymbol{u}) &= -\boldsymbol{\nabla} P + \boldsymbol{\nabla} \cdot \boldsymbol{\tau} \\
\frac{\partial \rho E}{\partial t} + \boldsymbol{\nabla} \cdot (\rho H \boldsymbol{u}) &= -\boldsymbol{\nabla} \cdot \dot{\boldsymbol{q}} + \boldsymbol{\nabla} \cdot (\boldsymbol{\tau} \boldsymbol{u}) + \boldsymbol{\nabla} \cdot \left(\rho \sum_{s=1}^{ns} h_s \mathcal{D}_s \boldsymbol{\nabla} c_s \right)
\end{aligned}
$$

Governing Equations

- Extension from a single-species calorically perfect gas to a reacting mixture of thermally perfect gases requires species conservation equations and additional energy transport mechanisms.

$$\begin{aligned}
\frac{\partial \rho_s}{\partial t} + \boldsymbol{\nabla} \cdot (\rho_s \boldsymbol{u}) &= \boldsymbol{\nabla} \cdot (\rho \mathcal{D}_s \boldsymbol{\nabla} c_s) + \dot{\omega}_s \\
\frac{\partial \rho \boldsymbol{u}}{\partial t} + \boldsymbol{\nabla} \cdot (\rho \boldsymbol{u}\boldsymbol{u}) &= -\boldsymbol{\nabla} P + \boldsymbol{\nabla} \cdot \boldsymbol{\tau} \\
\frac{\partial \rho E}{\partial t} + \boldsymbol{\nabla} \cdot (\rho H \boldsymbol{u}) &= -\boldsymbol{\nabla} \cdot \dot{\boldsymbol{q}} + \boldsymbol{\nabla} \cdot (\boldsymbol{\tau} \boldsymbol{u}) + \boldsymbol{\nabla} \cdot \left(\rho \sum_{s=1}^{ns} h_s \mathcal{D}_s \boldsymbol{\nabla} c_s \right)
\end{aligned}$$

- Problem class may also require a multitemperature thermal nonequilibrium option.

$$\frac{\partial \rho e_V}{\partial t} + \boldsymbol{\nabla} \cdot (\rho e_V \boldsymbol{u}) = -\boldsymbol{\nabla} \cdot \dot{\boldsymbol{q}}_V + \boldsymbol{\nabla} \cdot \left(\rho \sum_{s=1}^{ns} e_{Vs} \mathcal{D}_s \boldsymbol{\nabla} c_s \right) + \dot{\omega}_V$$

Turbulence Modeling

- We model the effects of turbulence using the Spalart-Allmaras one-equation turbulence model:

$$\frac{\partial}{\partial t}(\bar{\rho}\nu_{\text{sa}}) + \frac{\partial}{\partial x_j}(\bar{\rho}\tilde{u}_j\nu_{\text{sa}}) = c_{b1} S_{\text{sa}} \bar{\rho}\nu_{\text{sa}} - c_{w1} f_w \bar{\rho}\left(\frac{\nu_{\text{sa}}}{d}\right)^2 + \frac{1}{\sigma}\frac{\partial}{\partial x_k}\left[(\mu + \bar{\rho}\nu_{\text{sa}})\frac{\partial \nu_{\text{sa}}}{\partial x_k}\right] + \frac{c_{b2}}{\sigma}\bar{\rho}\frac{\partial \nu_{\text{sa}}}{\partial x_k}\frac{\partial \nu_{\text{sa}}}{\partial x_k}$$

with closure terms

$$\mu_t = \bar{\rho}\nu_{\text{sa}} f_{v1}, \qquad f_{v1} = \frac{\chi^3}{\chi^3 + c_{v1}^3}, \qquad f_{v2} = 1 - \frac{\chi}{1 + \chi f_{v1}}, \qquad \chi = \frac{\nu_{\text{sa}}}{\nu},$$

$$f_w = g\left(\frac{1 + c_{w3}^6}{g^6 + c_{w3}^6}\right)^{1/6}, \qquad g = r + c_{w2}\left(r^6 - r\right), \qquad r = \frac{\nu_{\text{sa}}}{S_{\text{sa}}\kappa^2 d^2}.$$

Turbulence Modeling

- We model the effects of turbulence using the Spalart-Allmaras one-equation turbulence model:

$$\frac{\partial}{\partial t}(\bar{\rho}\nu_{\text{sa}}) + \frac{\partial}{\partial x_j}(\bar{\rho}\tilde{u}_j\nu_{\text{sa}}) = c_{b1}S_{\text{sa}}\bar{\rho}\nu_{\text{sa}} - c_{w1}f_w\bar{\rho}\left(\frac{\nu_{\text{sa}}}{d}\right)^2 + \frac{1}{\sigma}\frac{\partial}{\partial x_k}\left[(\mu + \bar{\rho}\nu_{\text{sa}})\frac{\partial \nu_{\text{sa}}}{\partial x_k}\right] + \frac{c_{b2}}{\sigma}\bar{\rho}\frac{\partial \nu_{\text{sa}}}{\partial x_k}\frac{\partial \nu_{\text{sa}}}{\partial x_k}$$

and source term

$$S_{\text{sa}} = \Omega + S_m, \; S_{m0} = \frac{\nu_{\text{sa}}}{\kappa^2 d^2} f_{v2}$$

where

$$S_m = \begin{cases} S_{m0}, & S_{m0} \geq -c_{v2}\Omega \\ \dfrac{\Omega(c_{v2}^2\Omega + c_{v3}S_{m0})}{((c_{v3} - 2c_{v2})\Omega - S_{m0})}, & \text{otherwise.} \end{cases}$$

Thermodynamics & Transport Properties

- Thermochemistry models must be extended for a mixture of vibrationally and electronically excited thermally perfect gases.

$$
\begin{aligned}
e^{\text{int}} =& e^{\text{trans}} + e^{\text{rot}} + e^{\text{vib}} + e^{\text{elec}} + h^0 \\
=& \sum_{s=1}^{ns} c_s e_s^{\text{trans}}(T) + \sum_{s=mol} c_s e_s^{\text{rot}}(T) + \\
& \sum_{s=mol} c_s e_s^{\text{vib}}(T_V) + \sum_{s=1}^{ns} c_s e_s^{\text{elec}}(T_V) + \sum_{s=1}^{ns} c_s h_s^0
\end{aligned}
$$

  Here we have assumed that $T^{\text{trans}} = T^{\text{rot}} = T$ and $T^{\text{vib}} = T^{\text{elec}} = T_V$
- Additional transport property models are required. In this work we use
  - species viscosity given by Blottner curve fits,
  - species conductivities determined from an Eucken relation,
  - mixture transport properties computed via Wilke's mixing rule, and
  - mass diffusion currently treated by assuming constant Lewis number.

Chemical Kinetics & Energy Exchange

Kinetics:

- we consider *r* general reactions of the form

$$N_2 + \mathcal{M} \rightleftharpoons 2N + \mathcal{M}$$
$$\ldots$$
$$N_2 + O \rightleftharpoons NO + N$$
$$\ldots$$

- When combined with forward and backward rates, these reactions produce the species source terms $\dot{\omega}_s$
- Presently, we use either CANTERA or an in-house library to provide these source terms.

Energy Exchange:

- Equilibration between the energy modes is modeled with a typical Landau-Teller vibrational energy exchange model with Millikan-White species relaxation times.
- Provides the vibrational energy source term $\dot{\omega}_V$

Chemical Kinetics

- We consider r general reactions of the form

$$N_2 + \mathcal{M} \rightleftharpoons 2N + \mathcal{M}$$
$$\ldots$$
$$N_2 + O \rightleftharpoons NO + N$$
$$\ldots$$

- The reactions are of the form

$$\mathcal{R}_r = k_{br} \prod_{s=1}^{ns} \left(\frac{\rho_s}{M_s} \right)^{\beta_{sr}} - k_{fr} \prod_{s=1}^{ns} \left(\frac{\rho_s}{M_s} \right)^{\alpha_{sr}}$$

where α_{sr} and β_{sr} are the stoichiometric coefficients for reactants and products

- The source terms are then

$$\dot{\omega}_s = M_s \sum_{r=1}^{nr} (\alpha_{sr} - \beta_{sr}) (\mathcal{R}_{br} - \mathcal{R}_{fr})$$

Energy Exchange

$$\dot{\omega}_V = \dot{Q}_v + \dot{Q}_{\text{transfer}}$$

Energy Exchange

$$\dot{\omega}_V = \dot{Q}_v + \dot{Q}_{\text{transfer}}$$

We adopt the Landau-Teller vibrational energy exchange model

$$\dot{Q}_s^{\text{tr-vib}} = \rho_s \frac{\hat{e}_s^{\text{vib}} - e_s^{\text{vib}}}{\tau_s^{\text{vib}}}$$

where $\hat{e}_s^{\text{vib}}$ is the species equilibrium vibrational energy and the vibrational relaxation time τ_s^{vib} is given by Millikan and White

$$\tau_s^{\text{vib}} = \frac{\sum_{r=1}^{ns} \chi_r}{\sum_{r=1}^{ns} \chi_r / \tau_{sr}^{\text{vib}}}, \quad \chi_r = c_r \frac{M}{M_r}, \quad M = \left(\sum_{s=1}^{ns} \frac{c_s}{M_s} \right)^{-1}$$

and

$$\tau_{sr}^{\text{vib}} = \frac{1}{P} \exp \left[A_{sr} \left(T^{-1/3} - 0.015 \mu_{sr}^{1/4} \right) - 18.42 \right]$$

$$A_{sr} = 1.16 \times 10^{-3} \mu_{sr}^{1/2} \theta_{vs}^{4/3}, \quad \mu_{sr} = \frac{M_s M_r}{M_s + M_r}$$

Vibrational Energy Production and Energy Exchange

$$\dot{\omega}_V = \dot{Q}_v + \dot{Q}_{\text{transfer}}$$

Vibrational Energy Production and Energy Exchange

$$\dot{\omega}_V = \dot{Q}_v + \dot{Q}_{\text{transfer}}$$

When molecular species are created in the gas at rate $\dot{\omega}_s$, they contribute vibrational/electronic energy at the rate

$$\dot{Q}_{vs} = \dot{\omega}_s \left(e_s^{\text{vib}} + e_s^{\text{elec}} \right)$$

so the net vibrational energy production rate is

$$\dot{Q}_v = \sum_{s=1}^{ns} \dot{\omega}_s \left(e_s^{\text{vib}} + e_s^{\text{elec}} \right)$$

Vibrational Energy Production and Energy Exchange

$$\dot{\omega}_V = \dot{Q}_v + \dot{Q}_{\text{transfer}}$$

When molecular species are created in the gas at rate $\dot{\omega}_s$, they contribute vibrational/electronic energy at the rate

$$\dot{Q}_{vs} = \dot{\omega}_s \left(e_s^{\text{vib}} + e_s^{\text{elec}}\right)$$

so the net vibrational energy production rate is

$$\dot{Q}_v = \sum_{s=1}^{ns} \dot{\omega}_s \left(e_s^{\text{vib}} + e_s^{\text{elec}}\right)$$

Combining terms yields the desired net vibrational energy source term

$$\dot{\omega}_V = \sum_{s=1}^{ns} \dot{Q}_s^{\text{tr-vib}} + \sum_{s=1}^{ns} \dot{\omega}_s \left(e_s^{\text{vib}} + e_s^{\text{elec}}\right)$$

Ablation Processes

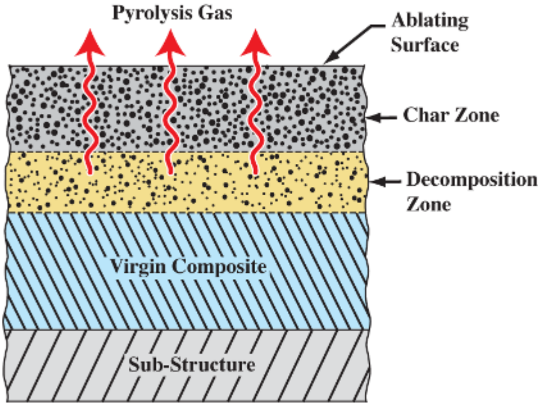

Schematic of ablation processes

- Ablation is a multi-scale, multi-physics phenomenon
- Sometimes amenable to simplification for predictive simulations

Quasi-steady State Ablation Hypothesis

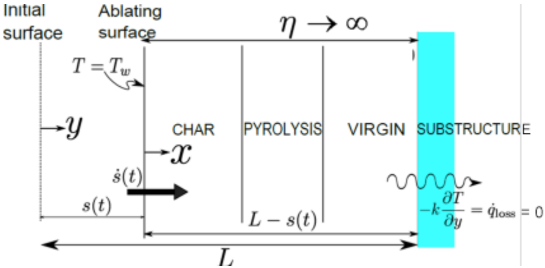

1. Steady state in reference frame fixed to the receding surface
2. Time variations solely due to motion of the material domain
3. Time scale for surface motion ($\dot{s} \approx 0.1 - 1$ mm/sec) much larger than characteristic time scale of unsteady processes
4. 1-D, semi-infinite medium

Quasi-steady Ablation

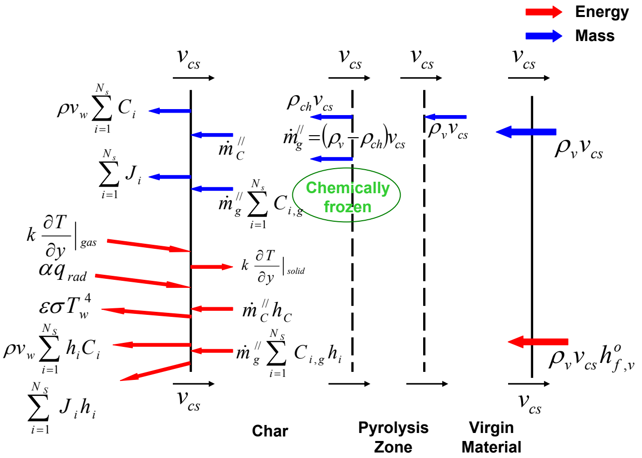

- Assumes ablation timescale $\ll$ trajectory timescale
- Assumes negligible substructure conduction

Ablation Interface Conditions

Recession:

$$\rho v_w = \dot{m}_c'' + \dot{m}_g''$$

Mass:

$$J_i|_{gas} + \rho v_w C_i = \tilde{N}_i(C_i, T) + \dot{m}_g'' C_{i,g}; (i : 1..N_s)$$

Energy:

$$- k\frac{\partial T}{\partial y}\bigg|_{gas} - \sum_{i=1}^{N_s} h_i(T_w)\, J_i|_{gas} + \dot{m}_c'' h_c(T) - \rho v_w h_w(T)$$

$$+\alpha \dot{q}_r'' - \sigma\epsilon {T_w}^4 + \sum_{i=1}^{N_s} \dot{m}_g'' C_{i,g} h_i(T_w) + k_s \frac{\partial T}{\partial y}|_{solid,w} = 0$$

- Nonlinear Robin Boundary Conditions
- Enables quasi-steady solves, restarts

Stabilized Finite Element Scheme

$$\frac{\partial \boldsymbol{U}}{\partial t} + \frac{\partial \boldsymbol{F}_i}{\partial x_i} = \frac{\partial \boldsymbol{G}_i}{\partial x_i} + \dot{\boldsymbol{\mathcal{S}}}$$

Stabilized Finite Element Scheme

$$\frac{\partial \boldsymbol{U}}{\partial t} + \boldsymbol{A}_i \frac{\partial \boldsymbol{U}}{\partial x_i} = \frac{\partial}{\partial x_i}\left(\boldsymbol{K}_{ij}\frac{\partial \boldsymbol{U}}{\partial x_j}\right) + \dot{\boldsymbol{\mathcal{S}}}$$

Stabilized Finite Element Scheme

$$\frac{\partial \boldsymbol{U}}{\partial t} + \boldsymbol{A}_i \frac{\partial \boldsymbol{U}}{\partial x_i} = \frac{\partial}{\partial x_i}\left(\boldsymbol{K}_{ij}\frac{\partial \boldsymbol{U}}{\partial x_j}\right) + \dot{\boldsymbol{\mathcal{S}}}$$

Find $\boldsymbol{U}$ satisfying the essential boundary and initial conditions such that

$$\int_\Omega \left[\boldsymbol{W}\cdot\left(\frac{\partial \boldsymbol{U}}{\partial t} - \dot{\boldsymbol{\mathcal{S}}}\right) + \frac{\partial \boldsymbol{W}}{\partial x_i}\cdot\left(\boldsymbol{K}_{ij}\frac{\partial \boldsymbol{U}}{\partial x_j} - \boldsymbol{A}_i\boldsymbol{U}\right)\right]\, d\Omega$$
$$+ \sum_{e=1}^{n_{el}} \int_{\Omega_e} \boldsymbol{\tau}_{\mathrm{SUPG}} \frac{\partial \boldsymbol{W}}{\partial x_k}\cdot\boldsymbol{A}_k\left[\frac{\partial \boldsymbol{U}}{\partial t} + \boldsymbol{A}_i\frac{\partial \boldsymbol{U}}{\partial x_i} - \frac{\partial \boldsymbol{G}_i}{\partial x_i} - \dot{\boldsymbol{\mathcal{S}}}\right]\, d\Omega$$
$$+ \sum_{e=1}^{n_{el}} \int_{\Omega_e} \nu_{\mathrm{DCO}}\left(\frac{\partial \boldsymbol{W}}{\partial x_i}\cdot g^{ij}\frac{\partial \boldsymbol{U}}{\partial x_j}\right)\, d\Omega - \oint_\Gamma \boldsymbol{W}\cdot(\boldsymbol{g} - \boldsymbol{f})\, d\Gamma = 0$$

for all $\boldsymbol{W}$ in an appropriate function space.

Stabilization Parameters

Discontinuity capturing operator:

$$\nu_{\text{DCO}} = \left[\frac{\left\| \frac{\partial \boldsymbol{U}}{\partial t} + \boldsymbol{A}_i \frac{\partial \boldsymbol{U}}{\partial x_i} - \frac{\partial}{\partial x_i} \left(\boldsymbol{K}_{ij} \frac{\partial \boldsymbol{U}}{\partial x_j} \right) \right\|^2_{\boldsymbol{A}_0^{-1}}}{(\Delta \boldsymbol{U}_h)^T \boldsymbol{A}_0^{-1} \Delta \boldsymbol{U}_h + g^{ij} \left(\frac{\partial \boldsymbol{U}_h}{\partial x_i} \right)^T \boldsymbol{A}_0^{-1} \frac{\partial \boldsymbol{U}_h}{\partial x_j}} \right]^{1/2}$$

SUPG stabilization matrix:

$$\boldsymbol{\tau}_{\text{SUPG}}^{-1} = \sum_{i=\text{nodes}} \left(\left| \frac{\partial \phi_i}{\partial x_j} \boldsymbol{A}_j \right| + \frac{\partial \phi_i}{\partial x_j} \boldsymbol{K}_{jk} \frac{\partial \phi_i}{\partial x_k} \right)$$

where

$$\left| \frac{\partial \phi_i}{\partial x_j} \boldsymbol{A}_j \right| = \boldsymbol{L} \left| \boldsymbol{\Lambda} \right| \boldsymbol{R}$$

Fully-Implicit Navier-Stokes (FIN-S)

Implementation Highlights

- C++ application code built on top of the `libMesh` library.
  - `libMesh` provides all requisite finite element data, parallel domain decomposition details.
  - Inherits PETSc preconditioned Krylov iterative solvers.
  - CANTERA used for kinetic rates, in-house thermodynamics, transport properties.
  - Only $\approx$ 30K SLOC
- Fully-coupled (monolithic solves), fully-implicit discretization.
- Rigorous verification using MASA-provided manufactured solutions.
- Testbed for intrusive VV/UQ schemes applied to hypersonics.

Spalart-Allmaras Perfect-Gas Verification

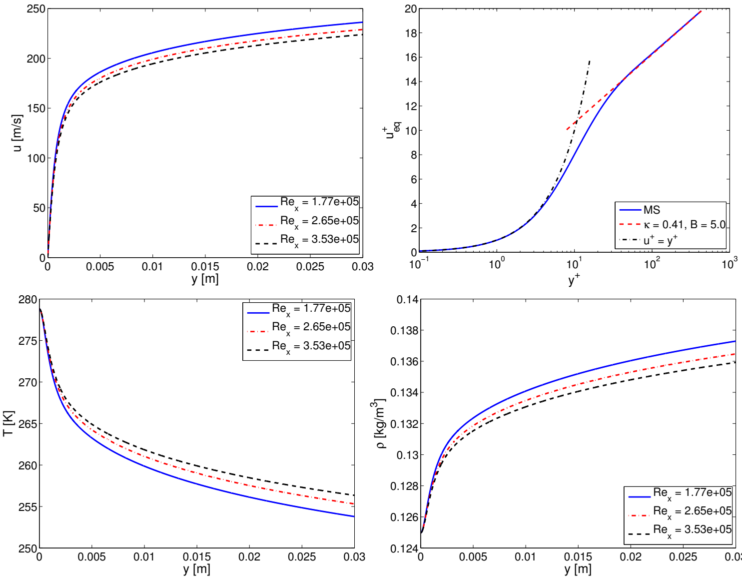

Spalart-Allmaras Perfect-Gas Verification

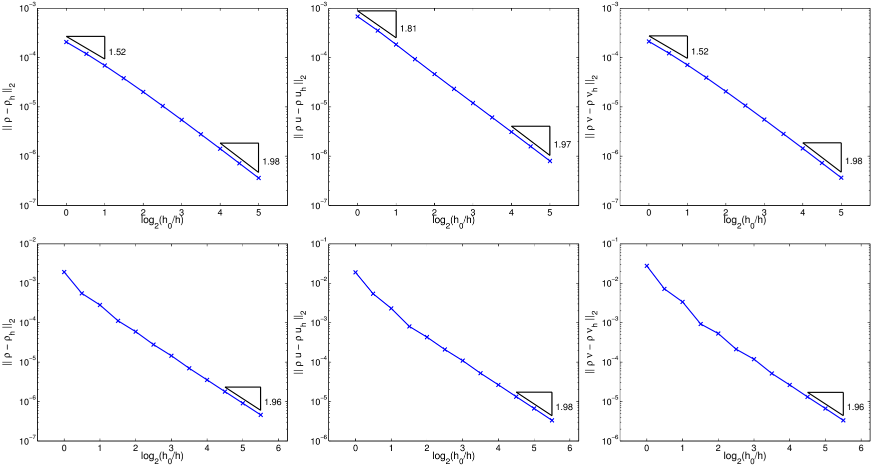

$\bar{\rho}$ $\bar{\rho}\tilde{u}$ $\bar{\rho}\nu_{\text{sa}}$

https://red.ices.utexas.edu/projects/software/wiki/MASA

Need for Parallelism

Large Problem Size

- Large numbers of unknowns.
  - For a Lagrange nodal basis:

$$\#\,\text{DOFS} = (\text{NS} + \text{NDIM} + \text{NE} + \text{NT}) \times \#\,\text{NODES}$$

  - Specifically, for our 13 species ablation model in 2D with turbulence

$$\#\,\text{DOFS} = (13 + 2 + 2 + 1) \times \#\,\text{NODES}$$

- For our implicit scheme, both storage and computational cost scale like $(\#\,\text{DOFS})^2$

Need for Parallelism

Complex Physical Models

- Chemical Kinetics, transport properties for NS species inherently expensive.
- Temperature is a nonlinear function of species concentration, internal energy for a mixture of thermally perfect gases.
- Quasi-steady ablation boundary condition is also nontrivial.

Opportunities for Parallelism

Multiple Types of Parallelism

1. **Domain Decomposition:** We use a standard non-overlapping domain decomposition approach provided by `libMesh`. Local computations are perfectly parallel, and the resulting implicit system is solved using preconditioned Krylov solvers from PETSc.
2. **Multithreaded Computation:** The relatively large element matrices resulting for reacting flows are well suited for threaded assembly. `libMesh` provides a convenient interface to Intel's Threading Building Blocks which can provide further parallelization on multicore architectures.
3. **Vectorization:** Remember vectorization? While no longer the *de facto* paradigm for high-performance computing, modern microprocessors offer vectorized instructions worth exploiting. We are using Eigen for dense linear algebra and inherit its SSE optimizations.

Domain Decomposition

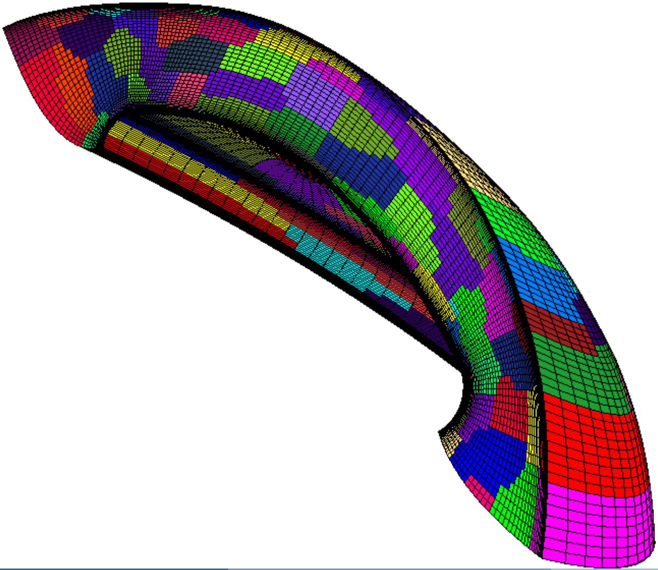

Domain Decomposition

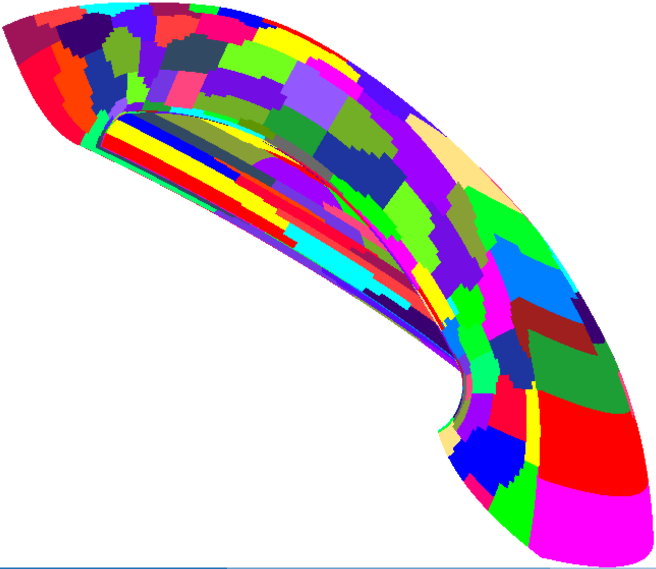

Speedup – Domain Decomposition

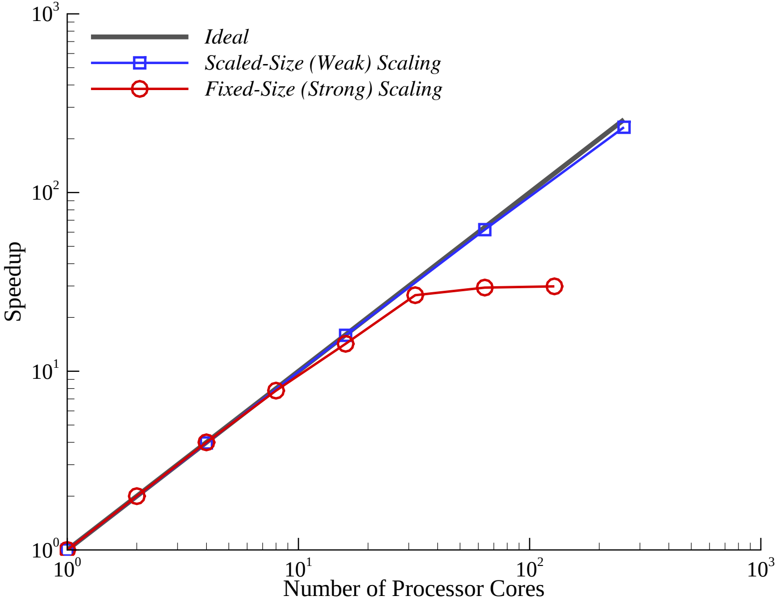

Multithreading

- Modern Parallel systems often contain 12–16 (or more) on-node cores connected via low-latency network.
- On-node multithreading allows an additional parallel mechanism that can extend scalability in certain circumstances.
- `libMesh` provides a clean interface to Intel®'s Threading Building Blocks (TBB) which is we have access to.
- TBB is a C++ template library consisting of
  - Algorithms
  - Containers
  - Mutexes
  - Timing routines
  - Memory allocators

  designed to help avoid low-level use of platform-specific (e.g. `pthread`) implementations.

Intel®'s Threading Building Blocks

- Requires more work than OpenMP but
  - Has better type-safety
  - Easier to reuse code
  - More natural for use with C++
- Once a standard `for` loop is selected for parallelization its components are abstracted as C++ `Range` and `Body` objects
- In FIN-S we parallelize matrix assembly, primitive variable computation, and other operations in this way.
  - Some operations perfectly asynchronous – e.g. computing primitive variables.
  - Other operations require locking shared objects – e.g. inserting local contributions to a global matrix.
  - Special care needed when interfacing with 3rd party libraries.

Speedup – Multithreading

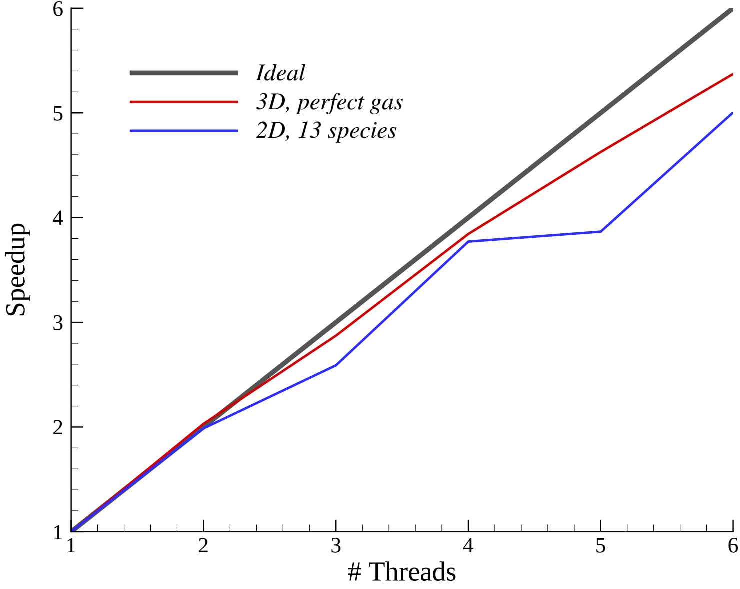

2D Extended Cylinder

- Laminar flow in thermal equilibrium
- Chemical nonequilibrium, 5 species air (N_2, O_2, NO, N, O)
- 5 reaction model with Park 1990 rates

$$
\begin{aligned}
c\mathrm{N}_{2,\infty} &= 0.78, c\mathrm{O}_{2,\infty} = 0.22 \\
U_\infty &= 6,731 \,\mathrm{m/sec} \\
\rho_\infty &= 6.81 \times 10^{-4} \,\mathrm{kg/m^3} \\
T_\infty &= 265\,\mathrm{K}
\end{aligned}
$$

- Blottner/Wilke/Eucken with constant Lewis number $Le = 1.4$ for transport properties
- Mesh, iterative convergence
- FIN-S/DPLR comparison

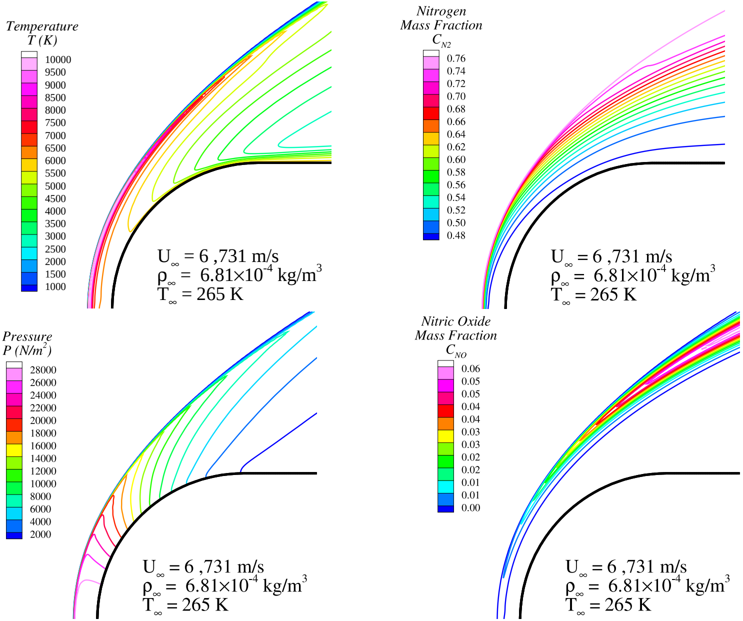
Temperature
T (K)
10000
9500
9000
8500
8000
7500
7000
6500
6000
5500
5000
4500
4000
3500
3000
2500
2000
1500
1000
U∞ = 6 ,731 m/s
ρ∞ = 6.81×10^-4 kg/m^3
T∞ = 265 K
Nitrogen
Mass Fraction
C_N2
0.76
0.74
0.72
0.70
0.68
0.66
0.64
0.62
0.60
0.58
0.56
0.54
0.52
0.50
0.48
U∞ = 6 ,731 m/s
ρ∞ = 6.81×10^-4 kg/m^3
T∞ = 265 K
Pressure
P (N/m^2)
28000
26000
24000
22000
20000
18000
16000
14000
12000
10000
8000
6000
4000
2000
U∞ = 6 ,731 m/s
ρ∞ = 6.81×10^-4 kg/m^3
T∞ = 265 K
Nitric Oxide
Mass Fraction
C_NO
0.06
0.05
0.05
0.04
0.04
0.03
0.03
0.02
0.02
0.01
0.01
0.00
U∞ = 6 ,731 m/s
ρ∞ = 6.81×10^-4 kg/m^3
T∞ = 265 K

Code-to-Code Comparison –
Stagnation Line

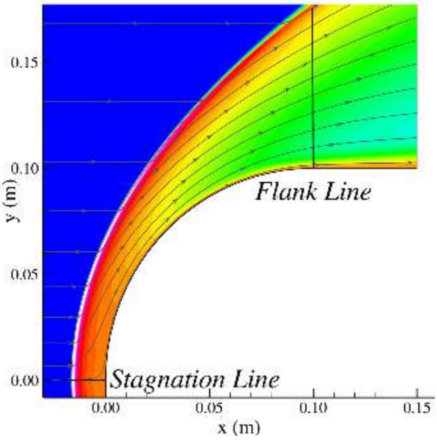

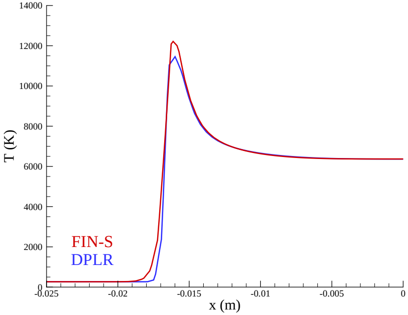

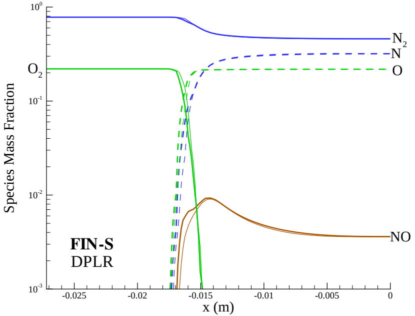

Code-to-Code Comparison –
Flank Line

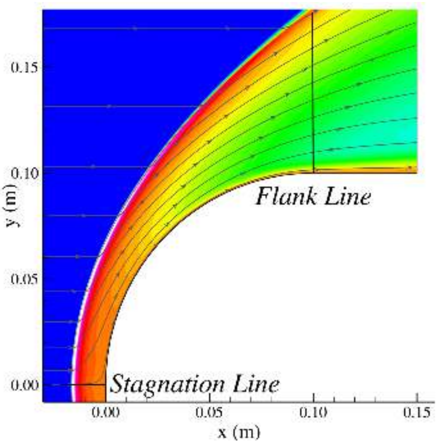

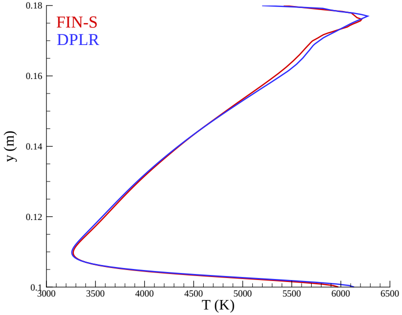

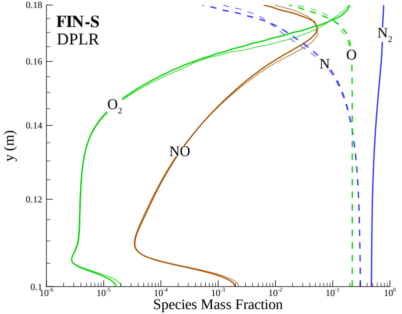

Mesh Convergence

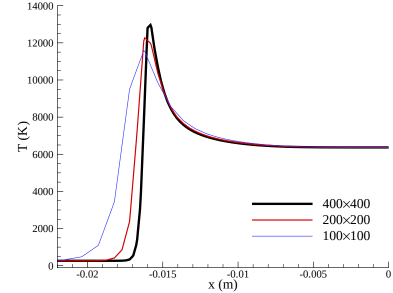

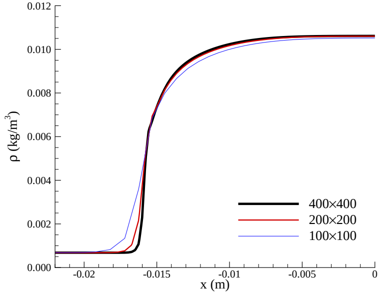

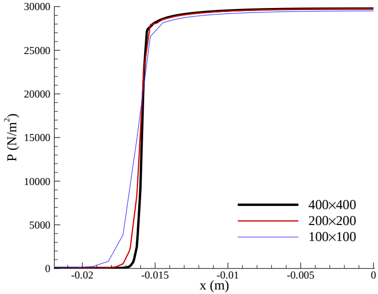

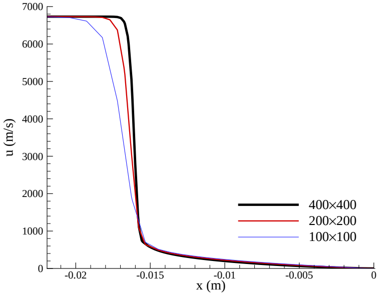

Iterative Convergence

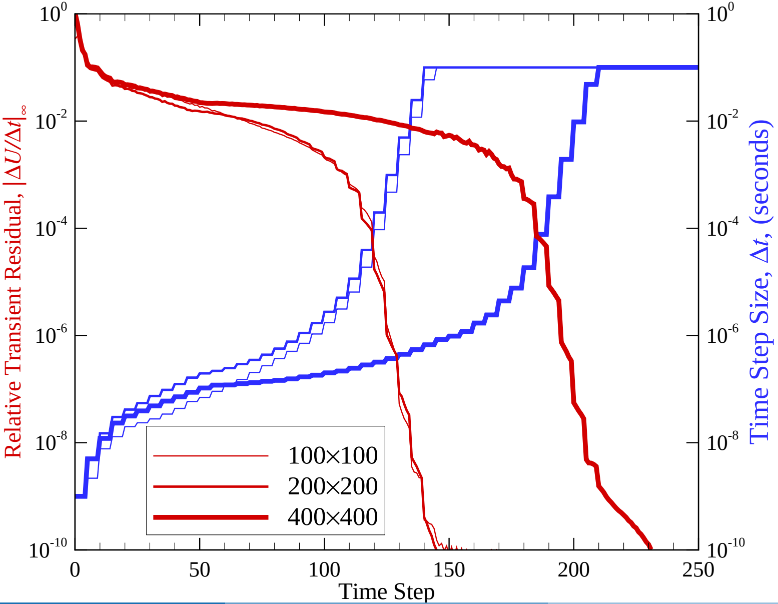

Ablating Boundary Experiments

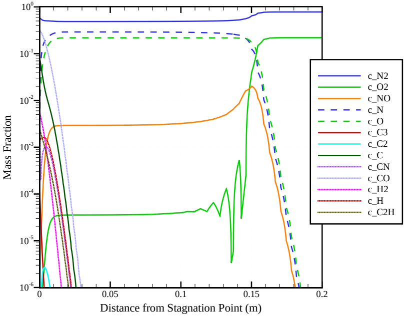

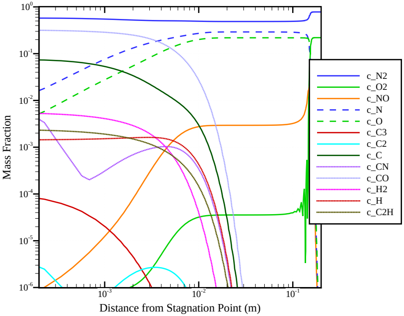

- Turbulent flow in thermochemical nonequilibrium, 13 species air (N_2, O_2, NO, N, O, C_3, C_2, C, CN, CO, H_2, H, C_2H), 18 reaction model with Park 2001 rates
- 5 Meter-scale domain, millimeter-scale chemical boundary layer

Ablating Boundary Experiments

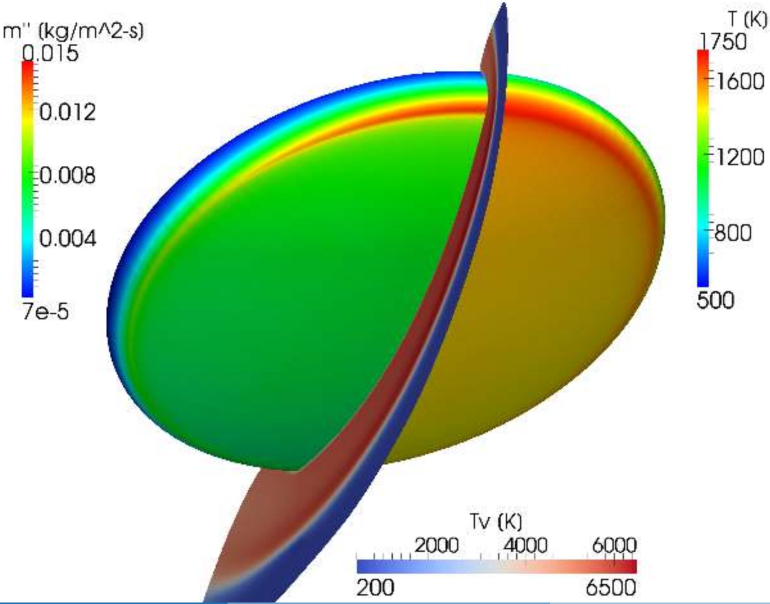

Arcjet Flowfields

Motivation

- Arcjets are uniquely suited to perform high enthalpy, long duration material response testing.
- Modern computational techniques are required to adequately characterize the freestream properties.
- Analysis complicated by multitude of scales, physical phenomenon:
  - Very low speed, high pressure plenum,
  - very high speed, low pressure nozzle exit,
  - highly nonequilibrium flow about test specimen.
- Adequately treating these phenomenon simultaneously is challenging for numerical methods.

Arcjet Flowfields

Arcjet Flowfields

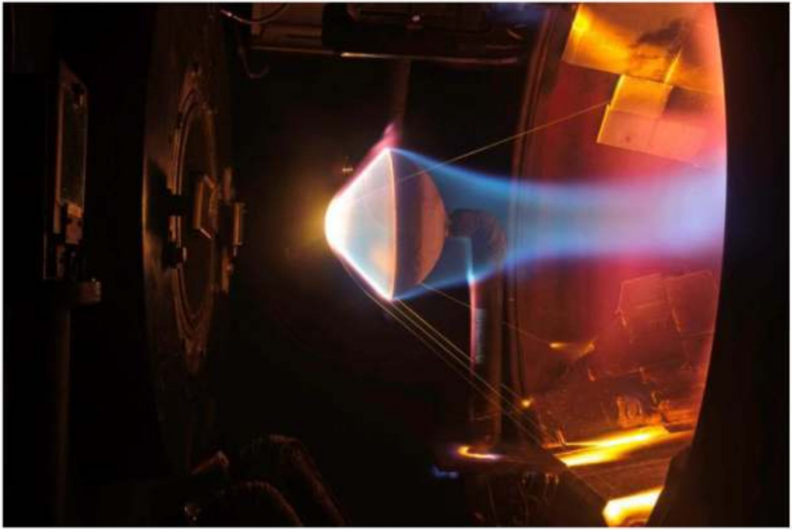

Arcjet Flowfields

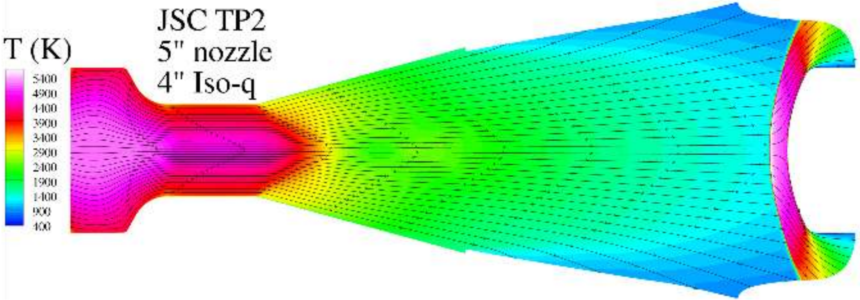

Arcjet Flowfields

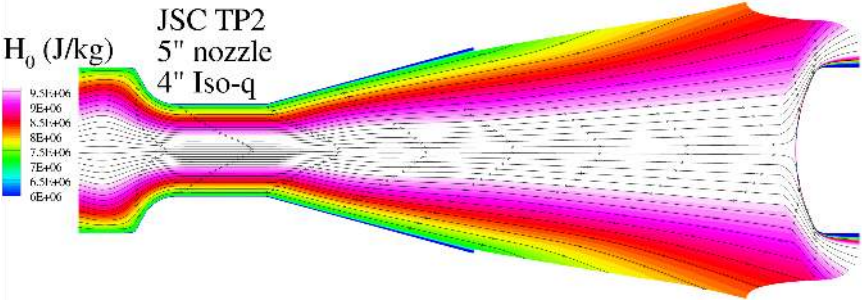

Full Disclosure

Opportunities for Further Enhancement

1. **Linear Solver Strategy:** Preconditioned GMRES is highly effective but potentially overkill for early, highly nonlinear transients. Mixed implicit/explicit schemes may provide a fast alternative.
2. **Improved Shock Capturing:** Robust shock capturing is still a challenge. Current scheme is fragile on bad meshes, and often convergence stalls.

Additional Focus Areas

1. Physics Modeling
   - Weakly Ionized Flows
   - Additional turbulence models
   - Fully coupled radiative transport
2. Unsteady ablation coupling
3. Adjoints
   - Sensitivity analysis
   - Adaptivity

Thank you!

Questions?